# *Pesquisas em Geociências*

*http://seer.ufrgs.br/PesquisasemGeociencias*

**Fine Euhedral Banding in Zircon - Metamorphic Enhacement of Igneous Structure**

*Léo Hartmann, Marcos Vasconcellos, Jayme Leite, Neal McNaughton*
*Pesquisas em Geociências,* 26 (1): 67-78, maio/ago., 1999.

Versão online disponível em:
*http://seer.ufrgs.br/PesquisasemGeociencias/article/view/21136*

Publicado por
**Instituto de Geociências**



Data de publicação - maio/ago., 1999.
Instituto de Geociências, Universidade Federal do Rio Grande do Sul, Porto Alegre, RS, Brasil

Pesquisas, 26 (1): 67-78, 1999
ISSN 0100-5375

Instituto de Geociências, UFRGS
Porto Alegre,RS-Brasil

# Fine Euhedral Banding in Zircon - Metamorphic Enhancement of Igneous Structure

LÉO A. HARTMANN[1]; MARCOS A. Z. VASCONCELLOS[2];
JAYME A. D. LEITE [1,3,4] & NEAL J. MCNAUGHTON[4]

[1] Instituto de Geociências, Universidade Federal do Rio Grande do Sul , Caixa Postal 15001
CEP 91509-900, Porto Alegre, RS, Brazil. afraneo@if1.if.ufrgs.br
[2] Instituto de Física,Universidade Federal do Rio Grande do Sul Caixa Postal 15051,
CEP 91501-970 Porto Alegre, RS, Brazil. marcos@if1.if.ufrgs.br
[3] Departamento de Recursos Minerais, Universidade Federal do Mato Grosso
CEP 78080-000 Cuiabá, MT, Brazil. jayme@cpd.ufmt.br
[4] Centre for Strategic Mineral Deposits, University of Western Australia,
Nedlands WA 6907 Australia. nmcnaugh@geol.uwa.edu.au

(Recebido em 03/99. Aceito para publicação em 06/99)

**Abstract** - Fine euhedral banding of zircon is usually considered to be associated with magmatic crystallization processes. This is commonly true, but it can also be generated by solid-state replacement along bands in previously more homogeneous crystals. Zircons from the Neoproterozoic Cambaí Complex in southernmost Brazil show abundant evidence to support solid-state replacement. Investigations of more than 135 zircon crystals by Electron Probe Microanalysis and Electron Backscattering techniques show that the solid-state replacement process begins along fractures and expands to broad irregular patches, even forming younger nucleii in some crystals. The replacement continues along crystallographically-controlled bands, enhancing and resembling fine oscillatory igneous zoning. Microprobe analyses indicate that modified zones are enriched in Y, U and Th in most BSE-bright bands, but in Hf in some others. The lighter (in BSE) parts in the core are texturally younger than the more homogeneous rims. The mechanisms involved include infiltration along fractures and defect sites and fluid-aided volume diffusion in less defective portions.

**Key words** - zircon, metamorphism, zoning, banding, geochemistry.

## INTRODUCTION

The internal structure of zircon crystals ranges from simple to complex. Zircons crystallized in a magma are commonly zoned, with fine euhedral zoning preserving the record of a complex evolution between crystallizing solid and liquid. Such regular zoning may extend from the innermost portions to the outermost rim of a crystal. Investigations by Vavra (1990, 1994), Halden & Hawthorne (1993), Benisek & Finger (1993) and Vavra *et al.* (1996) are well-documented studies of the internal morphology of zircon crystals.

Metamorphism can also recrystallize zircon grains or generate new ones. In extreme granulite-facies conditions, grains can appear homogeneous under the microscope or even in BSE images (Bertrand *et al.* 1992).

More complex situations may emerge under different natural conditions. For instance, partial melting of older crust followed by crystallization of the granitic melt may show zircons with an old homogeneous nucleus rimmed by finely zoned euhedral portions (Hanchar & Miller 1993) or an igneous, finely zoned core may be rimmed by a homogeneous metamorphic mantle (Pupin 1992).

Commonly a fine euhedral banding of zircon is attributed to magmatic crystallization. This interpretation is true for many zircons, but it is the purpose of this article to show examples where short-circuit and lattice diffusion generated euhedral bands in previously chemically more homogeneous crystals. We also show that cores can be chemically modified and investigate further the sealing of fractures previously described by Hartmann *et al.* (1997).

## DESCRIPTION OF SAMPLES

Four zircon crystals were selected for detailed electron probe micro-analysis (EPMA) and backscattered electron (BSE) studies out of a total of 130 crystals investigated in six rock samples previously studied by Leite *et al.* (1998) with Sensitive High Resolution Ion Micro Probe (SHRIMP) and BSE images. Nearly all grains show the textural aspects described in this paper, but the selected grains are

particularly helpful for the demonstration of the processes involved. Crystal 1 comes from a mafic meta-tonalite (RS-33-1), crystals 2 and 3 from a meta-trondhjemite (JL-1110) and crystal 4 from an amphibolite (JL-113). Fracture sealing in zircon crystals from this same meta-tonalite (RS-33-1) was previously described by Hartmann *et al.* (1997). All samples belong to the Cambaí Complex of Neoproterozoic age in Southernmost Brazil (Jost & Hartmann 1984; Babinski *et al.* 1996). They are part of the Cerro Mantiqueiras Ophiolite, strongly affected by deformation during middle amphibolite facies-grade metamorphism. Lower amphibolite facies retrogression is observed along shear zones, and some greenschist-facies overprint is also present; low temperature thermal effects of the Lavras granite are also observed.

Rock samples and zircon crystals show evidence of magmatic crystallization and regional metamorphism which were dated by Leite *et al.* (1998) in the age range 750-700 Ma with the zircon SHRIMP U/Pb method. This is the São Gabriel Orogeny of the Brasiliano Cycle. The four crystals discussed in the present work were also dated with one SHRIMP spot each, all of which plot close to concordia with less than 10 % discordance. The magmatic age of the tonalite was determined on six zircon crystals by Leite *et al.* (1998) at about 750 Ma. Three massive zircons with subrounded pyramidal terminations are concordant (% conc. <10%) and yield an age of about 700 Ma, interpreted as the age of regional metamorphism. It is significant that Remus *et al.* (1999) dated the volcanic eruption of the calc-alkaline andesitic Campestre Formation (50 km to the north of the studied area) at about 756 Ma and the regional metamorphism of this sequence at about 700 Ma. The magmatic and metamorphic ages are the same in these two infracrustal and supracrustal units of the São Gabriel Block.

Crystal 1 was selected after examination of 35 crystals by BSE imaging from more than 300 crystals initially observed under the optical microscope. Crystals 2 and 3 were selected out of 35 crystals evaluated by BSE imaging from a total of 312 crystals separated from this rock. Crystal 4 was selected after BSE imaging of 27 crystals from a total population of over 300 crystals from this rock sample, in which many crystals are broken.

## EXPERIMENTAL

EPMA analyses were performed in a CAMECA SX-50 at "Centro de Estudos em Petrologia e Geoquímica, Instituto de Geociências, Universidade Federal do Rio Grande do Sul, Brasil". One set of elements (U, Hf and Y) was selected to determine the spatial distribution of the elements in some banded regions as seen in BSE images because some of them are fairly abundant in zircon, whereas spatial profiles of another set of elements (U, Th and Pb) were also analyzed in order to relate their distribution with geochronological studies previously performed in these crystals.

Backscattering electron images (BSE) were all acquired with the following experimental conditions: accelerating voltage of 15 kV and current of 10 nA. Images were collected on Polaroid 55 paper and scanned. Re-polishing of crystal 2 was succeeded by the making of a new BSE image and profile analyses for U, Th and Pb.

Spaced profiles across banded regions and fractures observed in BSE images used 25 kV for the accelerating voltage of the electron beam, current of 10 nA and 1 μm diameter size beam. The profiles were acquired by moving the electron beam in steps of 0.5 μm in order to smooth the profiles. Lines used were Mα for U, Th and Pb and Lα for Y and Hf.

In order to transform the intensity of X-ray emission from each element to its concentration, characteristic X-ray emission lines were acquired in chosen points of the crystals and the quantification was made by supposing a linear relation between the concentration in the sample and in a standard. In the selected points, the characteristic emission lines for Hf, Y, Th, Pb and U were acquired using 25 kV, 100 nA and 50 sec per λ with steps of 0.0002 (in sin θ). Intensities for each element from the spot scan in the samples were compared with the same emission lines obtained from a known standard, using the same experimental conditions. No matrix corrections were used to determine the concentration in weight percent. Precision and accuracy of the results are approximately +/- 10% (1s). Standards used were synthetic $UO_2$, ThO, PbS and different synthetic glasses for U, Th, Pb, Hf and Y. It is important to emphasize that more than one standard was used for each element and the linear relation assumed was first used to compare results between standards, showing good agreement for the known concentrations (~10 wt%). Profiles $A_2$, $B_2$ and $C_2$ in crystal 2 for Th and Pb are shown in counts in figure 6 and not as wt% because Pb is near the detection limit and Th presents some uncertainties to generalize the values for intensity of background which shows deviations from point to point.

One hundred and eighty six spot analyses were made on 130 zircon crystals (Leite *et al.* 1998)) for U-Pb-Th isotopes at SHRIMP II facilities at Curtin University in Western Australia, following the procedures described by Compston *et al.* (1984) and more recently stated by Smith *et al.* (1998). Only the general age of 750-700 Ma is used in this paper, because

the magmatic crystallization and the metamorphic recrystallization occurred in a short time period of about 50 million years. The same SHRIMP mounts were used for EPMA studies in Brazil after re-polishing and carbon coating.

## BSE OBSERVATIONS

Figures 1, 2 and 3 are representative BSE images from a large set of images of zircon crystals from the three rock samples. Observation of these images shows that fractures are sealed in several zircon grains and that a bright signal is usually observed around the sealed regions. In addition, fine euhedral banding appears in cores and even in rims of the grains and bright bands start at the end of fractures. Below, we expand these observations.

The sealing of fractures described by Hartmann *et al.* (1997) is present in nearly all 130 crystals observed in the BSE images and is further demonstrated in figure 1 where crystal 1 shows several fractures partly or totally sealed by lighter gray zircon. Looked at in more detail (*a* in Fig. 1A), this fracture is sealed, although a ghost of the fracture can still be observed passing through the center of the very bright BSE signal (*a* in Fig. 1C). Fractures *b*, *c* and *d* in figure 1C terminate against bright (in BSE) portions (as seen in Fig. 1A) and are thus interpreted as entirely sealed at the two ends.

This sealing may expand away from the fractures to occupy a large central part of the crystals. This structure resembles and may be misidentified for an older core. Crystal 1 in figure 1 shows two such cores. The cores occupy a large volume of the grain, about 70%. One core is rounded and the other triangular in shape. The cores appear light gray in the BSE image, and may present some remnants of the older darker gray homogeneous crystal as seen, for instance, in point *b* of figure 1A. As seen in point *c* of figure 1A and point *e* of figure 1B, light gray material also occurs as a thin band close to the outermost rim, which may be generated by the same or by an unidentified process. The lower triangular core is continuous with the sealed fracture along a seam (sealed fracture) on point *f* of figure 1B. This seam is interpreted as a physical link between the sealed fracture and the new core; the presence of the bridge is understood as the path followed by the fluids as they entered the crystal and reached the core. The BSE images are of course a two-dimensional section of the complex three-dimensional array of interconnecting fractures, which served as pathways for the modification of the structure and composition of the crystal.

Many crystals from the Cambaí Complex also show fine euhedral banding in core regions. This would be commonly interpreted as a texture originated by igneous crystallization, followed by metamorphic homogenization of the rim. We propose an alternative description for the investigated crystals.

The formation of the fine euhedral banding was interrupted in crystals 2 and 3 (Fig. 2). In figures 2A and 2B, a remant homogeneous rim 10-20 μm thick is preserved along the lower and right side of the crystal. In figure 2A, a mineral inclusion 20 μm long straddles the boundary between the zoned and the unzoned portions of the zircon, indicating that the inclusion was present before the formation of the zoning. At point *a* in figures 2A and 2B, diffusion modified old zircon into new bright (in BSE) zircon starting from the end of the fracture; the two ends of the fracture seem discordant, and the bright (in BSE) band in between two may be new replaced zircon as well. The zoned structure might be misidentified as a finely euhedral, zoned remnant igneous core with a homogeneous metamorphic rim, but the image shows several fractures starting at the rim and sealed at the contact with a light gray band of the core region. These light gray bands have some curved boundaries, e.g. points *a*, *b* and *c* of figure 2C, but mostly follow crystallographic directions. Most important is the observation (point *d* in Fig. 2C) that the newly-formed band is euhedral and that it seals two fractures, which extend away from the two sides of the bright young band. This infiltration mechanism of sealing of fractures was studied previously by Hartmann *et al.* (1997). It is proposed that the homogeneous medium gray portions are remnant magmatic in composition, while the zoned bright (in BSE) portions had their chemistry modified by metamorphic fluids. In this manner, the crystalline magmatic structure of the zircon may remain unchanged, only the chemistry was modified. Only the relative age of formation of zircon can be determined in any specific crystal, commonly as medium gray (in BSE) magmatic portions and bright (in BSE) metamorphic portions. The absolute age determinations require ion microprobe isotopic investigations. Presumably, the two micro-structural types of zircon present in any single crystal corresponds to the two ages measured on the zircons of this rock by Leite et al. (1998).

Crystal 4 illustrates (Figs. 3A and 3B) a core and rim of homogeneous dark gray BSE signal. Between the two, a wide light gray euhedral mantle is newly formed, sealing several fractures. The mantle seals fractures in several places and remains overall euhedral.

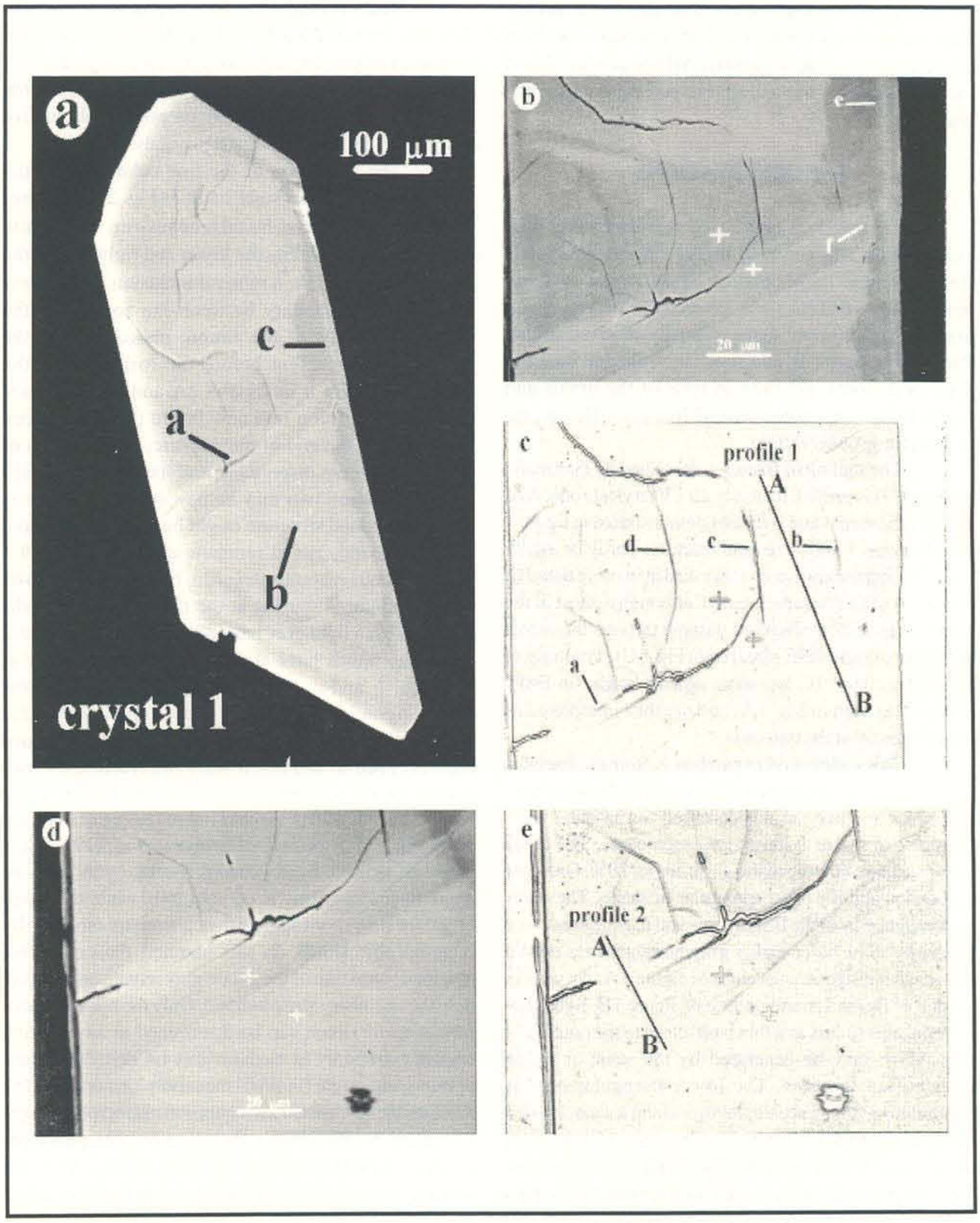


Figure 1 - BSE images and sketches of zircon crystal 1. (A): euhedral crystal; concentric, radial and longitudinal fractures present; sealed fractures in several places, such as *a*; dark portions preserved in the bright region at *b*; at *c*, the bright band is close to the rim; two large nucleii are present. (B): detail of (A). (C) sketch of (B), showing sealed fractures *a, b, c, d* and position of profile 1. (D) and (E): detail of (A) and corresponding sketch, showing position of profile 2.

## EPMA Hf, Y, U, Th, Pb

Scanning and spot WDS investigations were performed for U, Hf and Y on crystals 1, 3 and 4 to describe the chemistry of fracture sealing, core formation and euhedral banding. In addition, U, Th and Pb were analysed in crystal 3 for the investigation of this geochemical system which is much used in geochronology.

Profile 1 in figure 1C starts (Fig. 1B) at the border of the light gray upper core (core indicated by arrow), passes first through a dark gray part, then a light gray sealed fracture, another thin dark gray region and ends in the border region of the lower triangular light gray core (core indicated by arrow). There is a close relationship between brightness of band and chemistry (Fig. 4). It is well known (e.g. Hanchar & Miller, 1993; Hanchar & Rudnick, 1995) that intensity of BSE signal is proportional to mean atomic number. But for the elements investigated, the light gray parts are consistently enriched in Y, U, while Hf is enriched in the dark gray part.

Profile 2 in figure 1F runs from the darker region (Fig. 1D) through a sealed fracture, a narrow dark band and into the lower light gray core. The chemistry is coherent with profile 1 with a large increase in Y and U in the sealed fracture of profile 2 (Fig. 4). The light gray homogenized new core is strongly enriched in Y and impoverished in Hf.

Profile scannings were performed on crystal 3 and correspond to profiles 1a, 2a and 3a (Figs. 2E and 5). After repolishing, new profile scannings were performed approximately in the same position (profiles 1b, 2b, 3b in figure 6). All six profile scannings start at the core and pass through several light and dark gray bands. There is an overall decrease in Y, U and Th and increase in Hf from the lighter gray core region to the darker gray outer part. Observation of the BSE images (Figs. 2C, 2D and 2E) demonstrates that this light/dark gray relationship is well defined in several profiles and that there is good relationship between gray-tone contrast and chemistry. For instance, U and Th are very high in the core of profile 3b, coinciding with the intense brightness of the BSE signal in that portion. For comparison, U is fairly low in the core of profile 3a and only reaches comparable high values (*ca.* 0.1 wt%) at a distance of 15 μm from the core, again coinciding with the brightest (in BSE) portion. Pb is mostly below detection limit (*ca.* 0.02 wt%), but it was measured in profile 3b at 0.04 wt% in the same position where U reaches 0.12 wt% and Th increases to 0.25 wt%.

A thin (2-5 μm) dark (in BSE) external rim parallels the bright (in BSE) irregular portions that seal fractures between points *a* and *b* (Fig. 2C). This is a common feature of diffusional processes in zircon, as indicated by Hartmann *et al.* (1997, p. 68) and Silva *et al.* (1999) .

The observed decrease in Y and U from core to rim is the opposite of the more common behaviour reported for the igneous crystallization processes (Silver & Deutsch 1963), although it does occur when hornblende and titanite are extracted from the liquid. These elements (Y, Th and U) are usually incompatible and tend to concentrate in the remaining liquid from which the outer zones of the crystal form. So does Hf; Benisek & Finger (1993, p. 444) observed that "conventional magmatic processes operating during granite formation (e.g. fractional crystallization, new magma or fluid input etc.) do not provide realistic mechanisms for the fractionation of Hf versus Y and U in such an oscillatory fashion in the bulk melt". We consider it more likely that the three elements were not extracted from a liquid in the proportions now observed on the crystal. Melts in immediate contact with the growing crystal are unlikely to have the same compositon as the bulk melt, but we would expect the melts to evolve in chemically coherent manner. It is observed that the profiles in figures 5 and 6 are not equivalent to each other; if they represented cystallization from a magma, they should display similar compositions, for they are only twenty to fifty micrometers apart. A magmatic liquid would be expected to show much smaller compositional variation over this short distance. In cases where the crystal moves in a magma, the distance between the analysed faces is still small. It is also expected from igneous crystallization processes that the partition coefficient of trace elements between melt and crystal should oscillate in a limited range during crystallization; the profiles in figures 5 and 6 illustrate this oscillation between 0.02 and 0.1 wt % for U, 0.02 and 0.25 wt% for Th, 0.4 and 1.5 wt% for Hf, 0.2 and 0.6 wt% for Y. This oscillation is even more extreme in some parts of the profile. This feature is thus correctly explained by open-system diffusional processes and not by magmatic crystallization.

One profile was made across the sealed fracture at *a* in crystal 4 (Figs. 3a and 3b), and the dark gray portions were also analysed on either side. Here the sealed portion is enriched in U, Y too, and even in Hf, although Hf is higher in the dark, outer part of the crystal (Fig. 7).

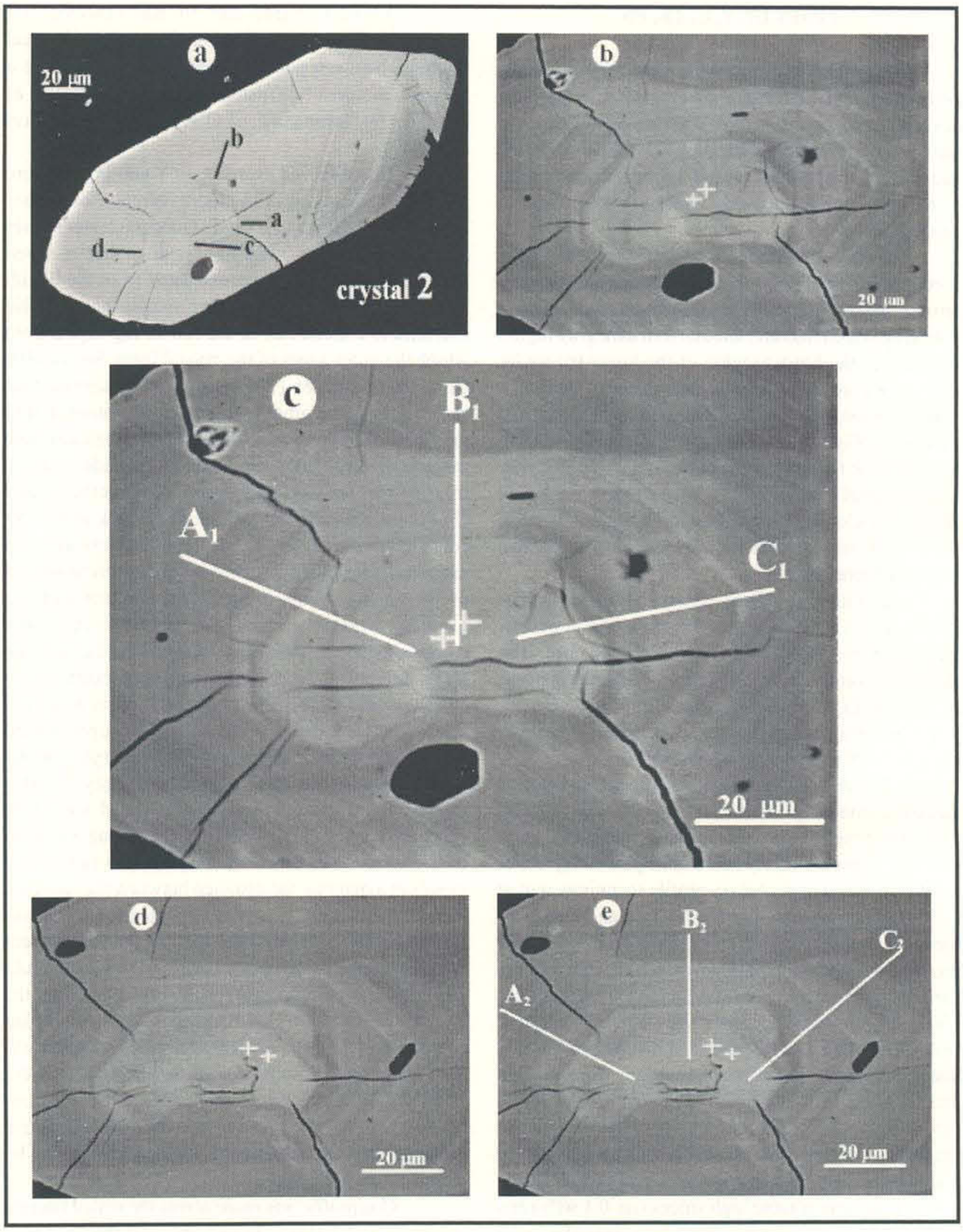


Figure 2 - BSE images of crystals 2 and 3. Euhedral crystal, showing radial and longitudinal fractures, and well developed euhedral banding; one inclusion of apatite is present in either crystal. In figures 2C, 2D and 2E, an irregular bright region is formed at *c* and at the end of a fracture at *a*, extends to *b*, and then accompanies the crystallographic structure towards *d*, where the euhedral band seals fractures. A thin dark (in BSE) band parallels the younger bright (in BSE) zircon from *a* to *b*. (D): detail of (C). (E): location of profiles on section seen on (D).

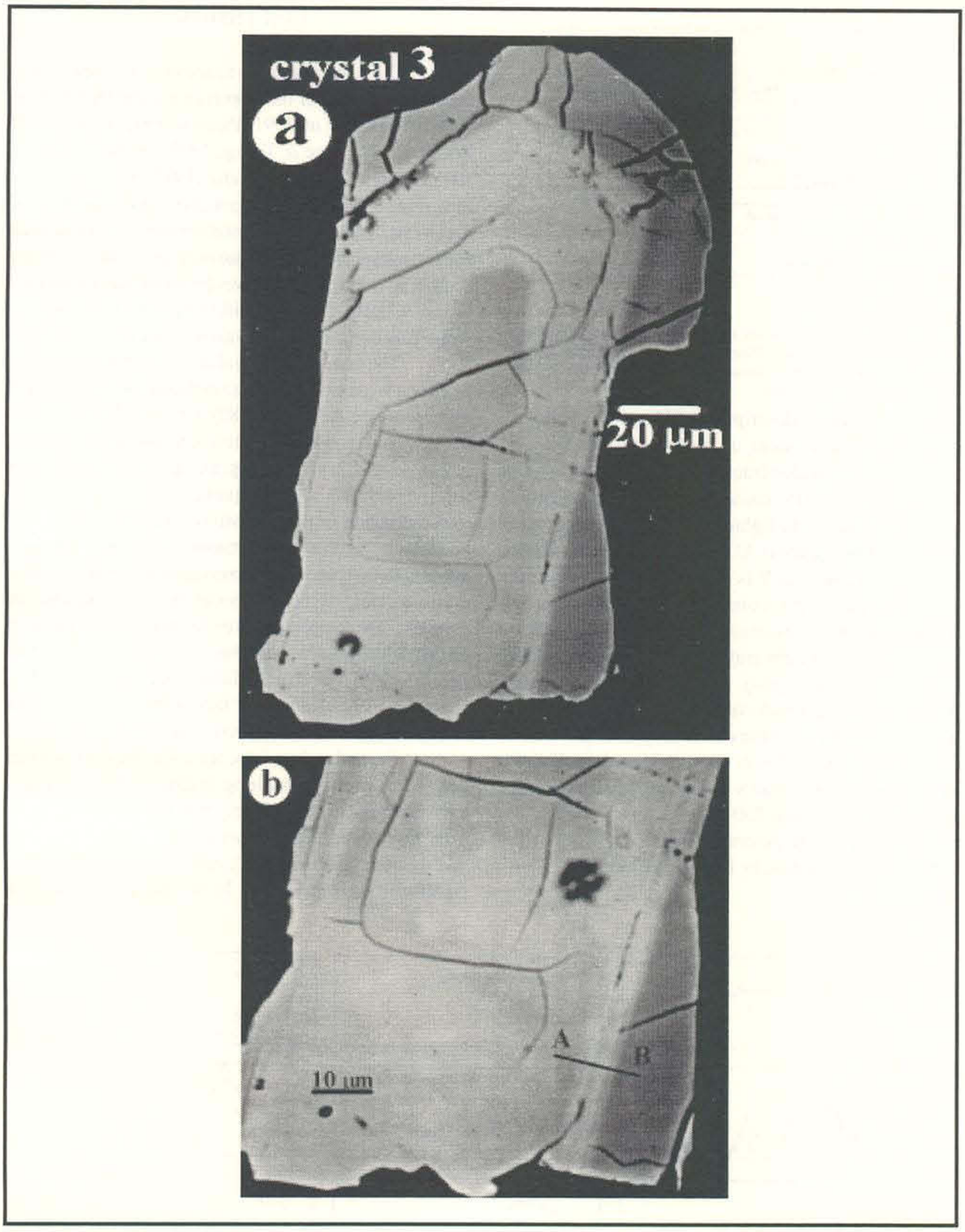


Figure 3 – BSE images of crystal 4. Euhedral crystal, showing radial, longitudinal and transversal fractures, partly sealed. (A) and (B): a bright band is seen to partly seal a fracture on the lower right and broaden upwards until it forms a large euhedral mantle in the upper part of the grain.

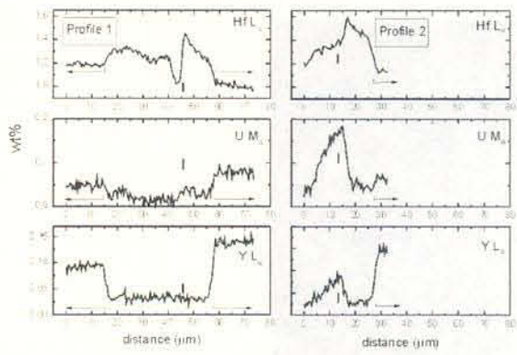


Figure 4 - Electron beam profiles representing the chemical distribution of Hf, U and Y in crystal 1. Position of young nucleii indicated by horizontal arrows; position of diffuse bright band – a sealed fracture – indicated by short vertical line.

The above description of U and Th chemistry shows that the content of these elements may be enriched in the sealed fracture by a factor of 5 (U) or 10 (Th) relative to the content in the dark gray parts of the crystal. But as the lighter gray parts become larger and more homogeneous, U is only enhanced by a factor of two. It seems that Y is irregularly enriched in the sealed fracture, but becomes strongly enhanced (5X) as the diffusion process reaches its final homogenization stage in the wider light gray parts. Hf is systematically high in the dark gray parts and lower in the homogenized light gray cores. Pb is not expected to be admitted into zircon from external sources because of its larger radius and lower charge. Therefore, high Pb in a few places is probably due to radioactive decay of U and Th over the last 700 Ma and not to introduction by diffusion from external sources, although this requires further testing by isotopic techniques.

## DISCUSSION

Different approaches to zircon studies have shown the complex nature of this important mineral (Kinny *et al.* 1988; Cherniak *et al.* 1991; Pidgeon, 1992; Pupin, 1992; Williams, 1992; Lee & Tromp, 1995; Roddick & Bevier, 1995; Elburg 1996; Hartmann *et al.*, 1997; Smith et al., 1998; Silva *et al.*, 1999). The high chemical and physical stability of zircon - the fact that a zircon crystal can survive many tectonic and metamorphic events and also many cycles of erosion and deposition - means that it preserves the record of a long geologic history. Clearly, the correct identification of the internal sequence of events of a zircon grain is essential for this purpose.

The external shape and the gross internal structure of zircon were extensively investigated with the optical microscope (e.g. Pupin, 1980). Other techniques have become more powerful for the understanding of complex crystals, and are now beginning to be used more intensively. As a consequence, the conditions of recrystallization or new growth of zircon are still poorly understood. For instance, Mattinson *et al.* (1996) conclude that "despite the abundance of observations of oscillatory zoning in zircons, there has been no comprehensive explanation of its origin." The complexities of the internal structure started to be unravelled with the systematic use of BSE images (Van Breemen, 1987; Hanchar & Miller, 1993; Vavra 1990, 1994; Silva *et al.*, 1999). In view of these studies, to what extent can zircon be considered a closed-system mineral?

Several authors have addressed the open-system behaviour of zircons along fractures. For instance, Chakoumakos *et al.* (1987, p. 1558) observed that "some of the fractures are filled with a material with a high uranium and thorium concentration", and they reached a rather significant conclusion (p. 1559) that "the system of

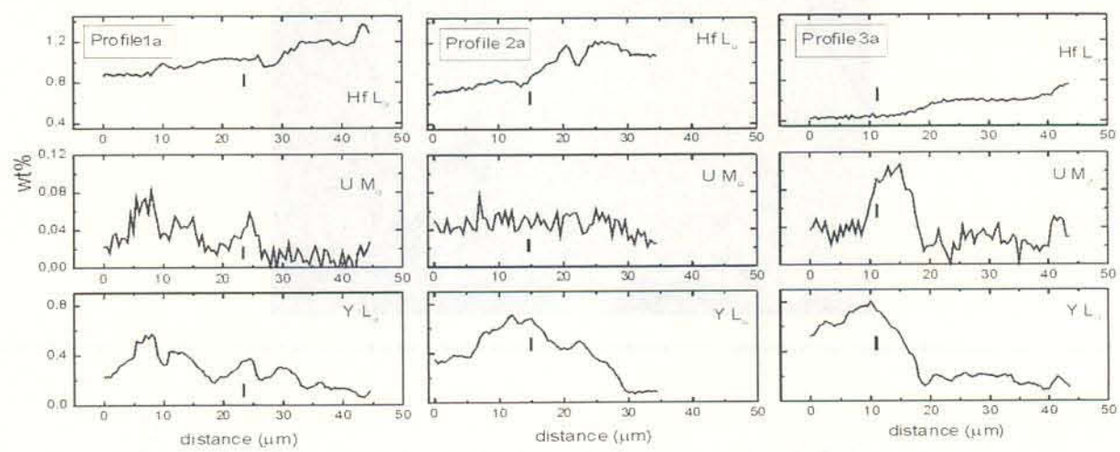


Figure 5 - Electron beam profiles representing the chemical distribution of Hf, U and Y in a section of crystal 3. Position of brightest band indicated by short vertical lines.

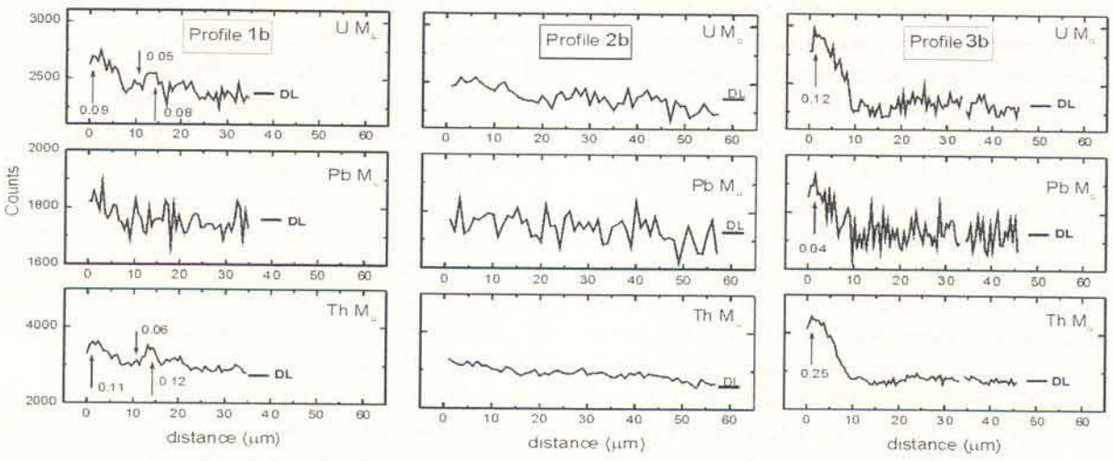


Figure 6 - Electron beam profiles representing the chemical distribution of U, Pb and Th in a deeper section (repolished) of crystal 3; profile approximately in the same position as the profiles from figure 5.

microfractures provides pathways for the addition or removal of uranium, thorium, and lead." Wayne & Sinha (1988, p. 111) concluded that the "healing of fractures may have taken place during the development of overgrowths, as new zircon coated fracture surfaces and grain perimeters." Heaman *et al.* (1990) and Hinton & Upton (1991, p. 3289) observed alteration with formation of new minerals along fractures in zircon. And also, Wayne *et al.* (1992, p. 414) observed that "...narrow zones of relatively high Z-number ... crosscut the concentric zoning pattern of the core. ... Microprobe analyses of one of the cross-cutting features ... indicates that its $HfO_2$ and $UO_2$ contents exceed, by a factor of 2, the highest observed concentrations of these in the core. This suggests that early fractures incurred by large zircon grains, perhaps during mylonitization, were subsequently healed by a later generation of Hf-U-rich zircon." Hanchar & Rudnick (1995, p. 298) observed that "nearly all of the zircons from this xenolith have what we infer to be paleo-fracturing with subsequent fluid-assisted filling of the fractures" and that "these filled fractures may indicate that the zircons were infiltrated with fluids from the surrounding environment". The studies of Zinger *et al.* (1996, p. 72) indicate that a "new zircon generation in the leucossomes of migmatites and weakly migmatized orthogneisses is discernible by CL in the form of substitutional structures along cracks..." And Claesson *et al.* (1997, p. 356), using high spatial resolution imaging, observed "... an intricate pattern of increased U concentration along major fractures which is superimposed on the magmatic zonation." In their study of Brazilian zircons, Hartmann *et al.* (1997, p. 71) concluded that "...fractures may occur irrespective of their position in the grain. Cores may be fractured and sealed anywhere within a crystal, so that younger material may occur within the crystal regardless of its prior igneous or metamorphic history."

Our investigations demonstrate further that the alteration produced by external fluids as they percolate along fractures in zircon may form large new cores and even new euhedral bands (Table 1). Actually, three closely-related structures were identified through the integrated use of BSE images, EPMA for Hf, Y and U quantification and SHRIMP isotopic studies. These three structures are the partial or total sealing of fractures by fluid infiltration, the extended fluid-aided diffusion of Hf, Y and U away from the fractures into broader regions until a large core is modified, and the fluid-aided diffusion of Y, U and Th into preferential bands with crystallographic control. We propose therefore that the generation of the euhedral banding corresponds to the metamorphic enhancement of the euhedral magmatic oscillatory zoning of the crystal. The enhancement of the internal structure of high-grade metamorphic zircon may also occur, but is less common, for these crystals are lower in U + Th and therefore less metamict.

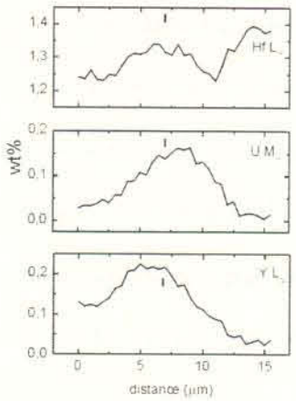


Figure 7 - Electron beam profiles representing the chemical distribution of Hf, U and Y in cristal 4. Fracture position indicated by short vertical line.

Zircon is a very stable mineral even under extreme geological conditions such as weathering, sedimentation, metamorphism and even partial melting (Paterson *et al.*, 1992; Williams, 1992; Vavra *et al.*, 1996). The closure temperature of zircon is usually considered close to 800°C (Heman & Parrish, 1990), but it is also known (Gebauer & Grünenfelder, 1976) that "temperatures of at most 350-400°C are sufficient to open U-Pb systems of metamict zircons or domains within zircons", because the concentration of fluid phases is more important than grade of metamorphism. Metamict zircon has a closure temperature of only 210°C for a crystal of 0.1 mm radius (Meldrum *et al.* (1998). Since all intermediate stages of metamictization may occur in zircons of different histories, the closure temperature can be seen as a rather variable attribute of zircons. High concentration of fluid phases will also enhance the diffusion rate of cations in zircon.

Oscillatory magmatic zoning in igneous zircons may be visible in CL images but is usually absent from BSE images due to low contrast in content of the heavy elements Hf, Y, and U. Only the very high variation in composition from one band to another caused by the introduction of the elements along more defective zones leads to the strong contrast in Z-number which is responsible for the strong intensity contrast observed in BSE images. In the sense of Halden & Hawthorne (1993, p. 1113), we consider very significant the "diffusion-controlled chemical feedback between the mineral and its environment" as a major cause of the strong oscillatory banding observed in many zircons, particularly in those subjected to complex geological events. Chemical modifications in zircons may proceed by diffusion inwards from the rims or outwards from the core as a mechanism of xenolithic zircon survival in crustal melts (Silva *et al.*, 1999).

Diffusion of these elements seems to be favoured in bands which were richer in U + Th originally and therefore were more defective due to α particle irradiation from U and Th. The ions probably diffused along bands by jumping from defect to defect in a fluid-aided diffusion process (Lee, 1993). Bands originally poorer in U were less defective and therefore had their chemistry better preserved. This explains the fine euhedral banding so strongly reminiscent of igneous zoning. Fluids responsible for the replacement were generated by regional metamorphism in the investigated samples.

Table 1 - Sequence of events recognized in Cambaí Complex zircon crystals.

| *Geological event* | *Feature on BSE image* |
|---|---|
| 1. Igneous crystallization | Homogeneous crystal, dull gray in BSE |
| 2. α-particle damage to the lattice in U-rich bands and portions | Unobserved (in BSE) variably metamictized bands |
| 3. Fractures are generated by crystal expansion and regional deformation | Fractures clearly observed (in BSE) |
| 4. Metamorphic fluids percolate and seal fractures, even in the cores of some crystals | Bright and/or dark U-rich paired bands |
| 5. Fluid-aided diffusion of ions through the defective parts of the lattice, adding U, Th and Y to fine oscillatory euhedral bands | Fine euhedral bright/dark (in BSE) banding reminiscent of igneous zoning (enhanced structure in BSE) and bright (in BSE) rounded, triangular or irregular new cores |

The presumed very low content of Y, U and Th in the fluid (ppb?) may have been sufficient for their capture and enrichment in the sealed fractures, younger cores and fine euhedral bands.

## CONCLUSIONS

Zircons from the Neoproterozoic Cambaí Complex in Southernmost Brazil were studied by EPMA and BSE techniques, after SHRIMP U/Pb isotopic investigations, and show that the solid-state replacement by fluid-aided diffusion begins along fractures and expands to broad irregular patches, even forming younger nucleii in some crystals. The replacement continues along crystallographically-controlled bands, enhancing the fine igneous zoning already present.

In some zircons, BSE images also demonstrate sealing of the fractures. EPMA analyses indicate that the new material is enriched in Y, U and Th in most bands and also in Hf in a few others. Older nucleii have been dated in many zircon crystals (Williams, 1992). But we suggest that this is not always the case, for the textural and chemical evidence in the investigated crystals favors the interpretation that some nucleii are younger than rims – old cores replaced by young cores due to diffusion of cations into zircon. The processes involved are related to fluid-aided diffusion of Y, U and Th through fractures and through defect sites in the lattice. These defects originated mostly from alpha-recoil damage during U and Th decay. Since these two elements are commonly zoned in zircon, the more enriched bands will be more defective and liable to replacement by new material. Important experimental evidence to support the interpretation include the high concentration of uranium around sealed fractures, the occurrence of high uranium bands at the end of fractures and a non-symmetrical band zoning unexplained from an igneous growth of the crystals.

In summary, our principal conclusions are:

1. Fine euhedral banding may be formed by fluid-aided diffusion processes, with similar composition in both the new bands and the sealed fractures;

2. Texturally younger homogeneous cores can be formed by solid-state diffusion;

3. The modified zircon which appears bright in BSE images is richer in Y, U and Th and poorer in Hf;

4. Ages of geological events in complex areas should only be determined after preliminary BSE study;

5. Fracture sealing is a common feature.

**Acknowledgments** - Conselho Nacional de Desenvolvimento Científico e Tecnológico (CNPq) of Brazil gave financial support for Jayme Leite's studies in Western Australia, and has supported Léo A. Hartmann's investigations. The electron microprobe laboratory at UFRGS was acquired and installed with PADCT/FINEP/UFRGS funds from the Brazilian Government. Paul Potter is thanked for the English review.

## REFERENCES

Babinski, M.; Chemale, F.; Hartmann, L.A.; Van Schmus, W.R. & Silva, L.C. da. 1996. Juvenile accretion at 750-700 Ma in Southern Brazil. **Geology**, **24**(5):439-442.

Benisek, A. & Finger, F. 1993. Factors controlling the development of prism faces in granite zircons: a microprobe study. **Contributions to Mineralogy and Petrology**, **114**:441-451.

Bertrand, J.M.; Roddick, J.C. & Allé, P. 1992. Comportement du zircon dans une zone de cisaillement granulitique (Orogène de Torngat, Protérozoïque inférieur du Labrador). In: Bertrand, J. M.; Barbey, P. & Chaudisson, M. 1992. **Zircon: morphologie et structure interne. Seminar at Vandoeuvre-les-Nancy, France** (unpublished).

Chakoumakos, B.C.; Murakami, T.; Lumpkin, G.R. & Ewing, R.C. 1987. Alpha-decay-induced fracturing in zircon: the transition from the crystalline to the metamict state. **Science**, **236**:1556-1559.

Cherniak, D.J.; Lanford, W.A. & Ryerson, F.J. 1991. Lead diffusion in apatite and zircon using ion implantation and Rutherford backscatering techniques. **Geochimica et Cosmochimica Acta**, **55**:1663-1673.

Claesson, S.; Andersson, U.B.; Schuhmacher, M.; Sunde, T.; Whitehouse, M. & Vestin, J. 1997. Inherited Archaean components in a Mesoproterozoic rapakivi complex from Central Sweden: implications from SIMS U-Pb imaging and spot analysis of zircon. In: EUG-9, European Union of Geosciences, Strasbourg. **Terra Nova**, **9**:356.

Compston, W.; Williams, I.S. & Meyer, C. 1984. Geochronology of zircons from the lunar breccia 73217 using a sensitive high mass resolution ion microprobe. **Journal of Geophysical Research**, **89**(supp. B):525-534.

Elburg, M.A. 1996. U-Pb ages and morphologies of zircon in microgranitoid enclaves and peraluminous host granite: evidence for magma mingling. **Contributions to Mineralogy and Petrology**, **123**:177-189.

Gebauer, D. & Grünenfelder, M. 1976. U-Pb zircon and Rb-Sr whole-rock dating of low-grade metasediments. Example: Montagne Noire (Southern France). **Contributions to Mineralogy and Petrology**, **59**:13-32.

Halden, N.M. & Hawthorne, F.C. 1993. The fractal geometry of oscillatory zoning in crystals - Application to zircon. **American Mineralogist**, **78**:1113-1116.

Hanchar, J.M. & Miller, C.F. 1993. Zircon zonation patterns as revealed by cathodoluminescence and backscattered electron images: Implications for interpretation of complex crustal histories. **Chemical Geology**, **110**:1-13.

Hanchar, J.M. & Rudnick, R.L. 1995. The application of cathodoluminescence and backscattered electron imaging to dating zircons from lower crustal xenoliths. **Lithos**, **36** (3/4):289-303.

Hartmann, L.A.; Takehara, L.; Leite, J.D.; McNaughton, N.J. & Vasconcellos, M.A.Z. 1997. Fracture sealing in zircon as evaluated by electron microprobe analyses and back-scattered electron imaging. **Chemical Geology**, **141**:67-72.

Heaman, L.M.; Bowins, R. & Crocket, J. 1990. The chemical composition of igneous zircon suites: Implications for geochemical tracer studies. Geochimica et Cosmochimica Acta, 54, 1597-1607.

Heaman, L. & Parrish, R. 1990. U-Pb geochronology of accessory minerals. *In*: Heaman, L. & Ludden, J.N. (ed.): **Applications of radiogenic isotope systems to problems in geology**. Short Course Handbook, Mineralogical Association of Canada, 19:59-102.

Hinton, R.W. & Upton, B.G. J. 1991. The chemistry of zircon: Variations within and between large crystals from syenite and alkali basalt xenoliths. **Geochimica et Cosmochimica Acta**, **55**:3287-3302.

Jost, H. & Hartmann, L.A. 1984. A Província Mantiqueira: Setor Meridional. *In*: Almeida, F.F.M. & Hasui, Y. (Ed.): **O Précambriano do Brasil.** Editora Edgard Blücher Ltda., São Paulo, Brazil, p. 365-368.

Kinny, P.D.; Williams, I.S.; Froude, D.O.; Ireland, T.R. & Compston, W. 1988. Early Archaen zircon ages from orthogneisses and anorthosites at Mount Narryer, Western Australia. **Precambrian Research, 38**: 325-341.

Lee, J.K.W. 1993. Problems and progress in the elucidation of U and Pb transport mechanism in zircon. *In*: Boland, J.N. &. Fitz Gerald, J.D. (Ed.): **Defects and Process in the Solid State: Geosciences Applications** (The McLaren Volume). Developmentos in Petrology, Elsevier Science Publishers, Amsterdam, **14**, 480 p.

Lee, J.K.W. & Tromp, J. 1995. Self-induced fracture generation in zircon. **Journal of Geophysical Research, 100**(B9):17,753-17,770.

Leite, J.A.D.; Hartmann, L.A.; McNaughton, N.J. & Chemale Jr., F. 1998. SHRIMP U/Pb zircon geochronology of Neoproterozoic juvenile and crustal-reworked terranes in southernmost Brazil. **International Geology Review, 40**: 688-705.

Mattinson, J.M.;Graubard, C.M.; Parkinson, D.L. & McClelland, W.C. 1996. U-Pb reverse discordance in zircons: the role of fine-scale oscillatory zoning and sub-micron transport of Pb. The American Geophysical Union, **Geophysical Monograph 95**:355-370.

Meldrum, A., Boatner, L.A., Weber, W.J., and Ewing, R.C. (1998) Radiation damage in zircon and monazite. **Geochimica et Cosmochimica Acta, 62**(14):2509-2520.

Paterson, B.A.; Stephens, W.E.; Rogers, G.; Williams, I.S.; Hinton, R.W. & Herd, D.A. 1992. The nature of zircon inheritance in two granite plutons. **Transactions of the Royal Society of Edinburgh: Earth Sciences, 83**:459-471.

Pidgeon, R.T. 1992. Recrystallization of oscillatory zoned zircon: some geochronological and petrological implications. **Contributions to Mineralogy and Petrology, 110**, 463-472.

Pupin, J.P. 1980. Zircon and granite petrology. **Contributions to Mineralogy and Petrology, 73**:207-220.

Pupin, J.-P. 1992. Les zircons des granites océaniques et continentaux: Couplage typologie-géochimie des élements en traces. **Bulletin Société Géologique de France, 163** (4), 495-507.

Remus, M.V.D.; McNaughton, N.J.; Hartmann, L.A.; Koppe, J.C.; Fletcher, D.I. & Pinto, V.M. 1999. Gold in the Neoproterozoic juvenile Bossoroca volcanic arc of southernmost Brazil: isotopic constraints on timing and sources. **Journal of South American Earth Sciences** (in press).

Roddick, J.C. & Bevier, M.L. 1995. U-Pb dating of granites with inherited zircon: Conventional and ion microprobe results from two Paleozoic plutons, Canadian Appalachians. **Chemical Geology, 119**:307-329.

Silva, L.C. da; Hartmann, L.A.; McNaughton, N.J. & Fletcher, I.R. 1999. SHRIMP U/Pb zircon timing of Neoproterozoic granitic magmatism and collision in the Pelotas Batholith in southernmost Brazil. **International Geology Review** (in press).

Silver, L.T. & Deutsch, S. 1963. Uranium-lead isotopic variations in zircons: a case study. **Journal of Geology, 71**:721-758.

Smith, J.B.; Barley, M.E.; Groves, D.I.; Krapez, B.; McNaughton, N.J.; Bickle, M.J. & Chapman, H.J. 1998, The Scholl shear zone, West Pilbara: Evidence for a terrane boundary structure from integrated tectonic analyses, SHRIMP U/Pb dating and isotopic and geochemical data of granitoids: Precambrian Research, v. 88, p. 143-171.

Van Breemen, O.; Henderson, J.B.; Loveridge, W.D. & Thompson, P.H. 1987. U-Pb zircon and monazite geochronology and zircon morphology of granulites and granite from the Thelon Tectonic Zone, Healey Lake and Artillery Lake map areas, N.W.T. In: **Geological Survey of Canada, Current Research, Part A, Paper 87-IA**:783-801.

Vavra, G. 1990. On the kinematics of zircon growth and its petrogenetic significance: a cathodoluminescence study. **Contributions to Mineralogy and Petrology, 106**:90-99.

Vavra, G. 1994. Systematics of internal zircon morphology in major Variscan granitoid types. **Contributions to Mineralogy and Petrology, 117**:331-344.

Vavra, G.; Gebauer, D.; Schmid, R. & Compston, W. 1996. Multiple zircon growth and recrystallization during polyphase Late Carboniferous to Triassic metamorphism in granulites of the Ivrea Zone (Southern Alps): an ion microprobe (SHRIMP) study. **Contributions to Mineralogy and Petrology, 122:**337-358.

Wayne, D.M. & Sinha, A.K. 1988. Physical and chemical response of zircons to deformation. Contributions to Mineralogy and Petrology, 98, 109-121.

Wayne, D.M.; Sinha, A.K. & Hewitt, D.A. 1992. Differential response of zircon U-Pb isotopic systematics to metamorphism across a lithologic boundary: an example from the Hope Valley Shear Zone, southeastern Massachusetts, USA. **Contributions to Mineralogy and Petrology, 109**:408-420.

Williams, I.S. 1992. Some observations on the use of zircon U-Pb geochronology in the study of granitic rocks. **Transactions of the Royal Society of Edinburgh. Earth Sciences, 83**:447-458.

Zinger, T.F.; Götze, J.; Levchenkov, O.A.; Shuleshko, I.K.; Yakovleva, S.Z. & Makeyev, A.F. 1996. Zircon in polydeformed and metamorphosed Precambrian granitoids from the White Sea Tectonic Zone, Russia: morphology, cathodoluminescence, and U-Pb chronology. **International Geology Reviews, 38**:57-73.